Toward the GMF for Wind Speed and Surface Stress Retrieval in Hurricanes Based on the Collocated GPS-Dropsonde and Remote Sensing Data

Olga Stanislavovna Ermakova, Daniil Alexandrovich Sergeev, Nikita Sergeevich Rusakov, Evgeny Ivanovich Poplavsky, Galina Nikolaevna Balandina, and Yuliya Igorevna Troitskaya

***Abstract*—This article describes the first step toward the development of the geophysical model function (GMF) for the retrieval of wind speed and wind stress in hurricanes, based on developing a relation between the cross-polarized satellite SAR data from Sentinel-1 and winds/stress observed from collocated NOAA GPS-dropsondes data. Field measurements and remote sensing data for tropical cyclones in the Atlantic Ocean were analyzed. Using the data measured by GPS-dropsondes, average wind velocity profiles were obtained, while the parameters of the wind boundary layer (drag coefficient and friction velocity) were restored from the "wake" part of the velocity profiles using the self-similarity property. The self-similarity of the velocity profile "defect" in the boundary layer, known from the fluid dynamics, was used to retrieve the parameters of the atmospheric boundary layer (the surface wind velocity, drag coefficient, and friction velocity) from the dropsonde wind velocity profiles in ten major hurricanes. Based on the processing of the measurements in the hurricanes Irma 2017/09/07 and Maria 2017/09/21 and 2017/09/23 at a time close to the time of acquisition of the Sentinel-1 images, the dependencies of the cross-polarized normalized radar cross section on the wind speed and wind friction velocity were obtained and used for constructing the GMFs.**

***Index Terms*—C-band, cross polarization, geophysical measurements, geophysics, hurricane, image analysis, radar cross sections, remote sensing, wind speed.**

I. Introduction

ACTIVE microwave remote sensing by the satellite-borne instruments is the most important state-of-the-art method of operational monitoring of the oceanic and atmospheric geophysical parameters. The main instruments for active microwave sensing of near-surface ocean winds are side-view radars (scatterometers), used to measure the signal backscattered from the sea surface [5], [10], [11], [16], [17], [19], [22], [24] in order to retrieve the wind speed and direction [10], [19] and the sea surface state. Their advantages are related to the possibility of all-weather 24-h global monitoring of the atmosphere and ocean state.

The first works on the use of active microwave methods for wind tangential turbulent stress, or wind friction velocity, retrieval have been presented recently (see, for example, [4], [13], [20], Liu, Tang, 2016). This approach seems preferable, since the small-scale roughness prescribing the magnitude of the backscattered signal is mainly related to the turbulent wind stress [13], and the dependence of the NRCS on the turbulent stress turns out to be stronger than on the wind speed (see, Jones and Schroeder, 1978, Weissman *et al.* 1994). Current turbulent stress retrieval algorithms use empirical geophysical model functions (GMFs) that associate NRCS with 10-m wind speed [7] and bulk formulas that relate wind speed U_{10} to the drag coefficient C_D. The dependence C_D (U_{10}) saturates at high wind speeds (>20 m/s, [6]) and is characterized by a peaking dependence [9], [14] during extreme wind conditions (>35 m/s).

Another problem of turbulent stress retrieval at strong winds is associated with the saturation of the scattered copolarized microwave signal at wind speeds exceeding 20 m/s [3], [21], [27]. Recently, a method has been proposed for solving this problem based on the cross-polarized scattered microwave signal reception. In this case, on the base of the field wind speed data analysis and water surface microwave SAR data, it was shown that the NRCS is sensitive to wind speed at high wind speeds [21], [25], [27]. Similar ground-based measurements of NRCS and turbulent surface stress do not exist. The present work is the first attempt to fill the existing gap. This article presents the first results of studies on the development of the dependency of NRCS on turbulent wind stress (or friction velocity) based on combined Sentinel-1 SAR data and field measurements of wind velocity profiles obtained by NOAA GPS-dropsondes in a wide range of weather conditions, including extremes. Friction velocity can be retrieved from the averaged over statistical ensemble wind velocity profiles using the Monin–Obukhov similarity (the

Manuscript received December 28, 2019; revised March 27, 2020 and July 13, 2020; accepted August 9, 2020. Date of publication August 18, 2020; date of current version August 28, 2020. This work was supported in part by the Russian Science Foundation under Project 19-17-00209 (collection and processing of remote sensing data) and in part by the Russian Foundation for Basic Research under Project 19-05-00249, Project 19-05-00366, and Project 18-35-20068 (collection and processing the data array of GPS-dropsondes, combining field data, and remote sensing data). The work of Olga Stanislavovna Ermakova was supported by the Ministry of Education and Science of the Russian Federation under Government Task 0030-2019-0020. The work of Daniil Alexandrovich Sergeev, Nikita Sergeevich Rusakov, Evgeny Ivanovich Poplavsky, Galina Nikolaevna Balandina, and Yuliya Igorevna Troitskaya was supported by Ministry of Education and Science of the Russian Federation under Government Task 0035-2019-0007. *(Corresponding author: Olga Stanislavovna Ermakova.)*

The authors are with the Department of Geophysical Research, Institute of Applied Physics of the Russian Academy of Sciences, Nizhny Novgorod 603155, Russia (e-mail: o.s.ermakova@mail.ru; daniil@hydro.appl.sci-nnov.ru; nikitarusakov228@yandex.ru; keepcalmandhavefun@mail.ru; fortune@appl.sci-nnov.ru; yuliya@hydro.appl.sci-nnov.ru).

Digital Object Identifier 10.1109/JSTARS.2020.3017704

profiling method). However, the profiling method cannot be directly applied to available GPS-dropsonde measurements for two reasons. The dominant one is extremely high measurement errors in the vicinity of the water surface. In addition, there is the problem of correct composition of the statistical ensemble for averaging [15]. In this article, we propose an approach to determine the law of resistance based on the approach successfully used in technical fluid dynamics to describe turbulent boundary layers over flat plates and tubes [8]. The method is concerned with the self-similarity of the velocity defect [see (1)] in the boundary layer, which makes it possible to retrieve the parameters of the boundary layer (friction velocity and the roughness height) from the measurements in the so-called "wake" part (the part where velocity dependence on height is parabolic and located above the logarithmic part), far from the surface. The advantage of this approach is the ability to use measurements of the air velocity profile at the distance from the surface, where there is a significantly larger amount of data. In addition, the deformation of the velocity profile due to wave momentum flux decreases with the distance from the surface (see, e.g., Kandaurov *et al.* 2014). This approach, applied to wind velocity profiles obtained from NOAA GPS-dropsonde data, is described in Section II. Section III discusses the algorithm for analyzing data from a Sentinel-1 satellite-based SAR measurement system to collocate GPS-dropsondes data available at the NOAA Hurricane Research Mission website[1] with remote sensing data. Section IV is devoted to the retrieval of the dependence of NRCS on turbulent wind stress (or friction velocity) based on a collocation of field data with available satellite data.

II. Statistical Analysis of Data From NOAA GPS-Dropsondes

The self-similar laws for velocity profiles in the turbulent boundary layer are applicable only to values averaged over a statistical ensemble. According to [15], the result of averaging is sensitive to the choice of a statistical ensemble. In the present study, a statistical ensemble comprises the wind velocity profiles measured under approximately the same conditions. It means that the velocity profiles were selected in a certain hurricane, at a certain day. The statistical ensemble was then formed from dropsondes that were closely spaced over a distance of approximately 10 km and demonstrating a similar dependence of wind speed on height.

Ten storms, categories 4 and 5 during 2003–2017 and during the Atlantic hurricane seasons, were selected for statistical analysis. The location of the GPS-dropsondes was related to the current position of the storm center according to the track data of the NOAA Hurricane Research Mission. The statistical ensembles of the velocity profiles are presented visually in the form of 3-D set of $U(R, z)$ curves in Fig. 1, where the members of the statistical ensembles are naturally combined into separate groups. We considered only the statistical ensembles of the profiles, where the wind speed at the upper boundary of the boundary layer exceeded 20 m/s (profiles marked in green in Fig. 1). The group of profiles measured in the hurricane eye (the red curves in Fig. 1) and at a considerable distance from the center of the hurricane with velocities at the upper boundary of the boundary layer less than 20 m/s (the blue curves in Fig. 1) were taken into consideration. As a result, the averaged wind velocity profiles were obtained [see Fig. 2(a)].

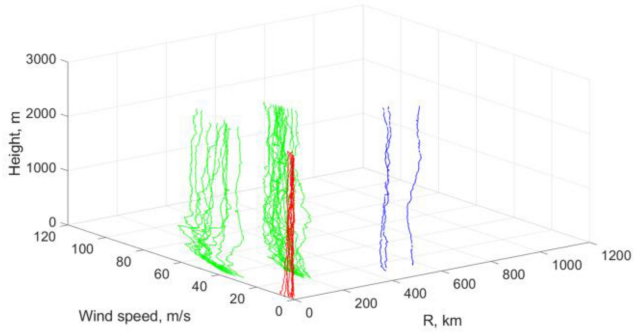

Fig. 1. 3-D illustrations. The axes, respectively, show the distance from the center of the hurricane (obtained by comparing the measurement data of the coordinates of the NOAA GPS-dropsondes and the coordinates of the hurricane's track at the moment of the dropsondes fall), wind speed, and altitude measured by the GPS sensor falling probe. Dataset for Hurricane Maria 2017/09/24.

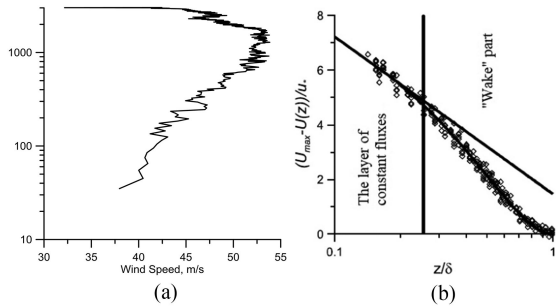

Fig. 2. (a) Example of a wind speed profile averaged over profile groups for the Hurricane Irma 2017/09/07. (b) Airflow velocity profiles measured in the aerodynamic flume at different wind speeds over the waves in self-similar variables. The solid line is logarithmic approximation. (Troitskaya *et al.* 2012.)

The planetary boundary layer in a storm, can to some extent, be treated as the flow in a channel, where the role of the upper lid is played by the capping inversion above the convective layer. In the turbulent boundary layers typical for the aerodynamic channels, three regions at different distances from the surface can be specified [see Fig. 2(b)]—the layer of constant fluxes with the logarithmic velocity profile and the "wake" part (parabolic dependence) (see [8]). The scale of the third viscous sublayer located near the surface is several orders of magnitude less compared to the layers specified above, so it was not taken into account. According to [26], the constant flux layer thickness is $\sim 0.3\delta$, where δ is the thickness of the turbulent boundary layer. In the storm boundary layer, the "wake" part is located above the layer of constant fluxes, where the boundary layer flow is adjusted to the geostrophic flow. The thickness of the planetary boundary layer in a storm is usually about 1000 m [see, e.g., Fig. 2(a)], which gives for the upper boundary of the layer of constant turbulent flux a thickness of $\sim$300 m. In the

[1][Online]. Available: http://www.aoml.noaa.gov/hrd/data_sub/hurr.html

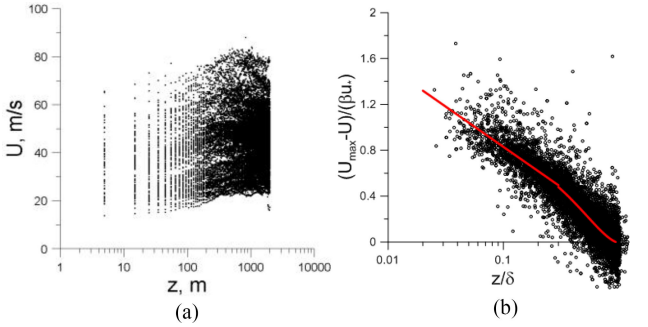

Fig. 3. Wind speed profiles in (a) dimensional variables and (b) self-similar variables. The red curve is an approximation by (5) with parameters determined by the least squares method.

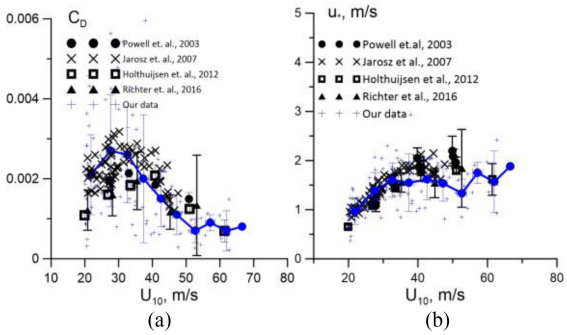

Fig. 4. Azimuth averaged dependences of (a) aerodynamic drag coefficient C_D and (b) dynamic wind speed u_* on U_{10}. The blue curve corresponds to the approximation of the obtained values at confidence intervals.

case of the waved water surface, the layer of constant fluxes contains the subregion where momentum is transferred from the airflow to wave disturbances at the water surface. In this subregion, the turbulent momentum flux changes with height and the velocity profile declines from logarithmic dependence, but the sum of the turbulent and wave momentum flux remains constant (Kandaurov *et al.* 2014). According to Makin *et al.* 1995, the scale of this region is about $\lambda/10$. In hurricanes of categories 4 and 5, the lengths of the wind waves are 400–500 m, which gives the lower boundary of the layer of constant turbulent flux lengths of 40–50 m. Thus, the logarithmic approximation of the velocity profile is valid only in the narrow range of heights and the traditional profiling method for determining dynamic wind speed and roughness parameter based on the logarithmic approximation of velocity profiles can be applied only to the limited amount of the data measured by GPS-dropsondes. Moreover, wind speed values measured near the water surface demonstrate large errors concerned with hurricane conditions. These problems can be solved if one uses data obtained at a large distance from the underlying surface. A similar approach was applied for measuring friction velocity in the wind-wave flume [18]. The self-similarity property of the velocity defect profile was used [8]

$$\frac{U_{\max} - U(z)}{u_*} = F\left(\frac{z}{\delta}\right) \tag{1}$$

where $U_{\max}$ is the maximum velocity in the turbulent boundary layer and u_* is the friction velocity. According to [8], for a nongradient turbulent boundary layer on a flat plate or in a wind channel, the following approximation of the self-similar velocity profile is valid:

$$U_{\max} - U(z) = \begin{cases} u_*\left(-\frac{1}{\kappa}\ln(z/\delta) + \gamma\right); & z/\delta < 0.3 \\ \beta u_*(1 - z/\delta)^2; & z/\delta > 0.3. \end{cases} \tag{2}$$

where $\kappa = 0.4$ is the Karman constant.

Here, this approach is applied to retrieve the parameters of the atmospheric boundary layer in a hurricane. First, the self-similarity of wind velocity profiles was verified for the atmospheric boundary layer of a storm. The airflow velocity profiles averaged over the selected ensembles were approximated by (2). The data obtained below 40 m were eliminated. Fig. 3 shows the velocity profiles in the boundary layer expressed in physical variables $U(z)$ and z and in the self-similar variables $\frac{U_{\max}-U(z)}{\beta u_*}$ and $\frac{z}{\delta}$. Obviously, the velocity profiles expressed in self-similar variables have much smaller spread than the initial ones and they are grouped around one curve. Approximation of the data in Fig. 3(b) by (2) gives $-1/(\kappa\beta) = 0.309$ and $\gamma/\beta = 0.123$.

Given the self-similarity of the airflow velocity profile, it is possible to obtain the parameters of the logarithmic boundary layer from measurements in the wake part of the turbulent boundary layer. The parameters of the logarithmic boundary layer are calculated by (2) for $z/\delta < 0.3$ as follows:

$$U(z) = \frac{u_*}{\kappa}\ln(z/z_0), \quad z_0 = \delta\exp\left(-\kappa U_{\max}/u_* + \frac{\gamma}{\beta}\kappa\right). \tag{3}$$

The expression for the aerodynamic drag coefficient then follows from (2)

$$C_D = \frac{\kappa^2}{\left(\kappa U_{\max}/u_* - \alpha\kappa + \ln(H_{10}/\delta)\right)^2} \tag{4}$$

where H_{10} is height 10 m above the sea level.

The dependencies of the drag coefficient and friction velocity on wind speed obtained in this way are shown in Fig. 4.

It should be noted that here we obtained the azimuth averaged values similar to those obtained by [9] and [14]. Similarly, at $U_{10} > 30$ m/s, the drag coefficient decreases with the wind speed increase. It should be emphasized that the proposed modified profiling method for determining the parameters of the atmospheric boundary layer enables the use of data measured at a large distance from the underlying surface. This makes it possible to utilize a much larger amount of data than within the traditional profiling method which is applicable only to the limited dataset acquired near the water surface where measurements have a large error. This approach makes it possible to reduce the number of wind velocity profiles necessary for averaging and retrieving the parameters of the atmospheric boundary layer (in particular, u_*) from data acquired in a certain hurricane at a certain time. Then, the wind velocity profiles measured at a time close to the time of acquisition of satellite SAR data can be used for calibration not only by the wind velocity, but also by the friction velocity. This makes it possible in prospect to construct

the novel geophysical model function (u_*-GMF), namely, NRCS via the friction velocity of the wind flow.

III. Sentinel-1 Satellite Remote Sensing Data Analysis

The above results were used to develop the u_*-GMF based on using the collocated remote sensing data from the Sentinel-1 satellite and field measurements obtained from GPS-dropsondes. We used the data acquired by C-SAR radar of the satellite Sentinel-1 (European Space Agency) operating at a frequency of 5.405 GHz. The interferometric wide swath mode was analyzed for images acquired during the hurricane season 2017 (from June 1, 2017 to November 30, 2017) over the Atlantic Ocean at VH cross polarization. The analysis of the SAR data showed that the records of the hurricane eye were acquired only for three hurricanes: Irma [2017/09/03–2017/09/10, Category 5 (SSHS)], Maria [2017/09/18–2017/09/27, Category 5 (SSHS)], and Jose [2017/09/09–2017/09/20, Category 4 (SSHS)]. It should be noted that in contrast to the Earl hurricane (2010), for which special ground measurements were carried out,[2] the special collocated measurements for these hurricanes were absent. Investigation of the possibility of collocation of the SAR data and the NOAA GPS-dropsondes for the hurricane season 2017 in the Atlantic Ocean showed that the data can only be collocated for the hurricanes Irma (2017/09/07) and Maria (2017/09/21 and 2017/09/23), since the image of the hurricane eye and measurements from GPS-dropsondes were the closest in time and space.

For each image, we analyzed the array of measurement data from GPS-dropsondes collocated with it in time and space. It should be noted, however, that the GPS-dropsondes were launched for a rather long period (6–10 h), not always coinciding exactly with the time of the image acquisition. Therefore, we assume that there is a certain period of time during a full-fledged cyclone for which some of its characteristics can be considered quasi-stationary. To verify this assumption, we analyzed the dynamic characteristics of hurricanes—minimum sea level pressure (MSLP) and maximum surface wind speed (MWS) (see Fig. 5). It can be seen that during the launch of GPS-dropsondes, these characteristics change slightly. It makes possible the collocation of satellite data and the data from GPS-dropsondes during this period.

In this regard, an array of data from GPS-dropsondes, launched 36 h before and after the time the image, was selected for analysis, while conserving of the hurricane dynamic characteristics was controlled. The GPS-dropsonde data was collected and arrays were divided into groups constructed from closely spaced GPS-dropsondes. Within each of these groups, the profiles measured by GPS-dropsondes were averaged. From the averaged profiles, the values of the wind friction velocity and the 10-m wind speed were obtained based on the procedure described above.

Preprocessing of the selected satellite images in the specialized software SNAP[3] included calibration and thermal noise and speckle noise removal. It should be noted, however, that significant fluctuations of the NRCS in each image were associated with the presence of surface waves. To reduce these fluctuations, the NRCS were averaged linearly over the square area $2 \times 2\,\text{km}^2$ with the centers in the points with the coordinates of the launched GPS-dropsondes. Afterward, we found the NRCS averaged over the ensemble of these points and then it was conversed to dB. Examples of such ensembles are shown in Fig. 6 inside red ellipses.

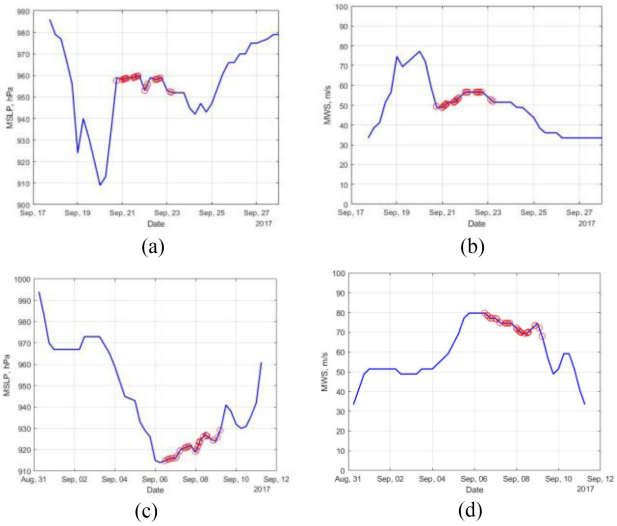

Fig. 5. Time dependence of MSLP for (a) Maria, (c) Irma and MWS for (b) Maria and (d) Irma. Red circles indicate the launch time of GPS-dropsondes.

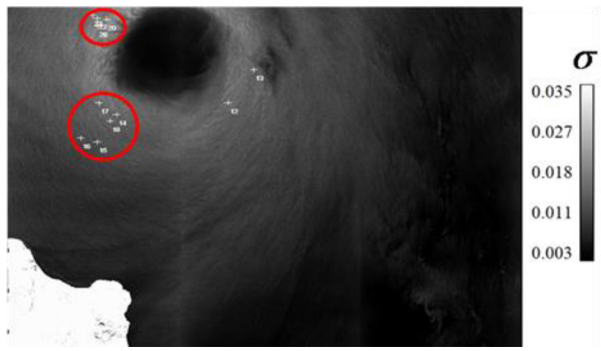

Fig. 6. Illustration of closely launched dropsonde groups. Radar image of the C-band from the satellite Sentinel-1 (2017/09/21); NRCS appears as the brightness characteristic. The analysis was conducted during the period 2017/09/20–2017/09/22.

The NRCS values versus the parameters of the atmospheric boundary layer (the 10-m wind speed, wind friction velocity) are shown in Fig. 7(a) and (b). For comparison, we used an array of data obtained on cross polarization in a wide range of wind speeds by Hwang *et al.* [11]. In [20], the authors used data from [11] to retrieve the dependence of the NRCS on u_*. Obviously, Fig. 7(a) shows that the present datasets are in agreement with the dependence from [11] and extend it to higher wind speed.

At the same time, it is seen from Fig. 7(b) that the dependence of NRCS on u_* becomes ambiguous for $u_* \approx 2$ m/s. An analysis of dependency [u_*on U_{10}, see Fig. 7(c)] and GPS-dropsondes

[2][Online]. Available: http://www.aoml.noaa.gov/hrd/Storm_pages/earl2010/sfmr.html

[3][Online]. Available: https://step.esa.int/main/toolboxes/snap/

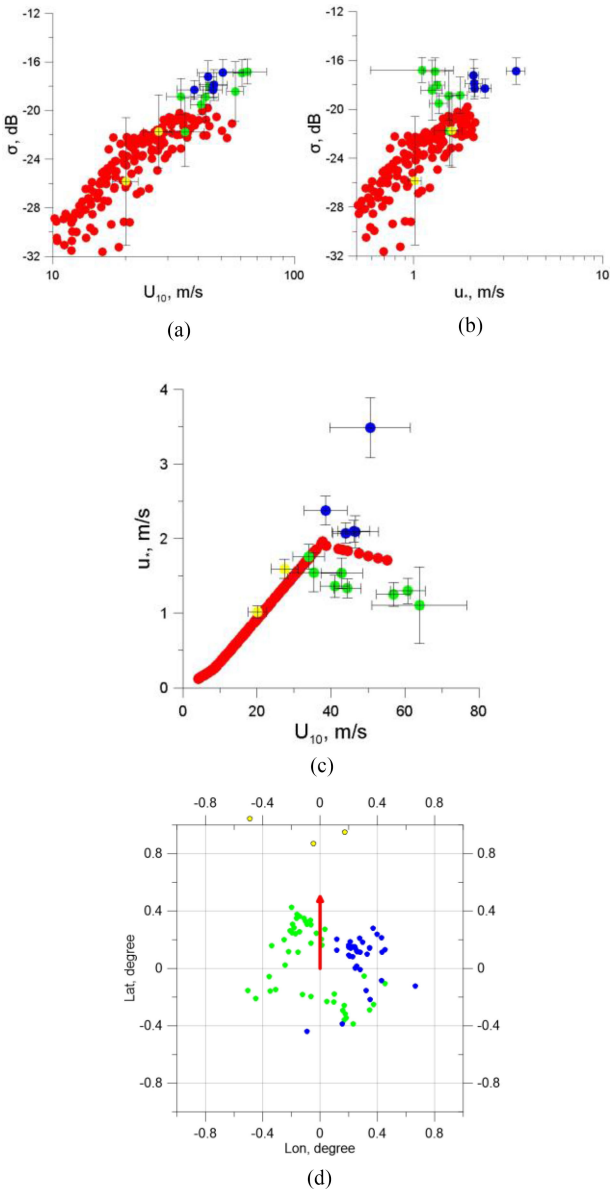

Fig. 7. NRCS dependency on (a) U_{10} and (b) u_*, and (c) u_* dependency on U_{10} in hurricanes Maria and Irma, obtained on the basis of collocated satellite data and measurement results from NOAA GPS-dropsondes analysis. (a) and (b) Red symbols indicate the NRCS obtained according to the data from [11] and [20]. (c) Red symbols show functional dependencies from [9] and [20]. Green and blue symbols show data obtained from left and right sector of hurricane, respectively. Yellow symbols indicate data from GPS-dropsondes fallen far from the hurricane center. (d) Illustration of sectoral distribution of data in hurricanes Maria and Irma, where red arrow shows the direction of hurricanes' motion.

distribution [see Fig. 7(d)] showed that the data corresponding to different branches of the dependence belong to GPS-dropsondes fallen in left and right sectors of the hurricanes. It should be noted that for data obtained far from the center of the hurricane (yellow symbols in Fig. 7), where wind speeds are low, the sectoral dependence is not so obvious.

IV. Conclusion

This article describes the first step toward the development of GMF for retrieval of wind speed and wind stress in hurricanes based on calibration of the cross-polarized satellite SAR data from Sentinel-1 by the collocated NOAA GPS-dropsondes data. The self-similarity of the velocity profile "defect" in the boundary layer, known from the fluid dynamics, was used to retrieve the parameters of the atmospheric boundary layer (the surface wind velocity and the wind friction velocity) from the GPS-dropsonde wind velocity profiles in ten major hurricanes. The advantage of this approach is the ability to use measurements of the velocity profile at a distance from the surface, which enhance the data ensemble and reduce the measuring errors. In addition, a procedure was proposed for selecting a statistical ensemble for averaging the GPS-dropsondes data as groups of wind velocity profiles measured under similar conditions. On the basis of the proposed approach, the parameters of the boundary layer (friction velocity and roughness height) were restored for the hurricanes of the Atlantic Basin in the period from 2003 to 2017. A procedure for collocation of the GPS-dropsondes data and the Sentinel-1 cross-polarized SAR data acquisition was suggested, based on the assumption that the shape of the hurricane remains unchanged during the time of field measurements. Based on preliminary data processing, the dependencies of the cross-polarized NRCS on the wind speed U_{10} and wind friction velocity u_* were obtained. The dependence on U_{10} is in agreement with the dependence from [11] and is extended to higher wind speed. The NRCS dependence on u_* is ambiguous apparently due to dependency of u_* on the sector of the hurricane. The found peculiarities are the subject of further investigation. First of all, further studies with the better statistics of the data are needed for constructing GMF for retrieving u_* from the remote sensing data.

References

[1] W.-K. Chen, *Linear Networks and Systems*. Belmont, CA, USA: Wadsworth, 1993, pp. 123–135.

[2] M. A. Donelan *et al.*, "On the limiting aerodynamic roughness of the ocean in very strong winds," *Geophys. Res. Lett.*, vol. 31, no. 18, Sep. 2004, Art. no. L18306, doi: 10.1029/2004GL019460.

[3] W. J. Donnelly *et al.*, "Revised ocean backscatter models at C and Ku band under high-wind conditions," *J. Geophys. Res., Oceans*, vol. 104, no. C5, pp. 11485–11497, May 1999, doi: 10.1029/1998JC900030.

[4] O. S. Ermakova, D. A. Sergeev, G. N. Balandina, N. S. Rusakov, E. I. Poplavsky, and Y. I. Troitskaya, "Retrieval of atmospheric boundary layer parameters in a tropical cyclone based on the collocated data from GPS-sondes and satellite radar images," *Sovr. Probl. DZZ Kosm.*, vol. 16, no. 6, pp. 51–59, 2019.

[5] D. Fernandez, J. R. Carswell, S. Frasier, P. S. Chang, P. G. Black, and F. D. Marks, "Dual-polarized C- and Ku-band ocean backscatter response to hurricane-force winds," *J. Geophys. Res., Oceans*, vol. 111, Aug. 2006, Art. no. C08013, doi: 10.1029/2005JC003048.

[6] R. J. Foreman and S. Emeis, "Revisiting the definition of the drag coefficient in the marine atmospheric boundary layer," *J. Phys. Oceanogr.*, vol. 40, pp. 2325–2332, Oct. 2010, doi: 10.1175/2010JPO4420.1.

[7] H. Hersbach, A. Stoffelen, and S. de Haan, "An improved C-band scatterometer ocean geophysical model function: CMOD5," *J. Geophys. Res., Oceans*, vol. 112, Mar. 2007, Art. no. C03006, doi: 10.1029/2006JC003743.

[8] J. O. Hintze, *Turbulence: An Introduction to Its Mechanism and Theory*. 1st ed. New York, NY, USA: McGraw-Hill, 1959. p. 586.

[9] L. H. Holthuijsen, M. D. Powell, and J. D. Pietrzak, "Wind and waves in extreme hurricanes," *J. Geophys. Res., Oceans*, vol. 117, Sep. 2012, Art. no. C09003, doi: 10.1029/2012JC007983.

[10] J. Horstmann, D. R. Thompson, F. Monaldo, S. Iris, and H. C. Graber, "Can synthetic aperture radars be used to estimate hurricane force winds?," *Geophys. Res. Lett.*, vol. 32, Nov. 2005. Art. no. L22801, doi: 10.1029/2005GL023992.

[11] P. Hwang *et al.*, "Cross-polarization geophysical model function for C-band radar backscattering from the ocean surface and wind speed retrieval," *J. Geophys. Res.*, vol. 120, pp. 893–909, Feb. 2015, doi:10.1002/2014JC010439.
[12] E. Jarosz , D. A. Mitchell , D. W. Wang, and W. J. Teague, "Bottom-up determination of air-sea momentum exchange under a major tropical cyclone," *Science*, vol. 315, pp. 1707–1709, Mar. 2007, doi: 10.1126/science.1136466.
[13] W. T. Liu and X. Xie, "Sea surface wind/stress vector," in *Encyclopedia of Remote Sensing*. New York, NY, USA: Springer, 2014, pp. 759–767.
[14] M. D. Powell, P. J. Vickery, and T. A. Reinhold, "Reduced drag coefficient for high wind speeds in tropical cyclones," *Nature*, vol. 422, pp. 279–283, Mar. 2003.
[15] D. H. Richter, R. Bohac, and D. P. Stern, "An assessment of the flux profile method for determining air–sea momentum and enthalpy fluxes from dropsonde data in tropical cyclones," *J. Atmos. Sci.*, vol. 73, no. 7, pp. 2665–2682, Mar. 2016, doi: 10.1175/JAS-D-15-0331.1.
[16] H. Shen, W. Perrie, and Y. He, "A new hurricane wind retrieval algorithm for SAR images," *Geophys. Res. Lett.*, vol. 33, Nov. 2006, Art. no. L21812, doi: 10.1029/2006GL027087.
[17] B. W. Stiles and R. S. Dunbar, "A neural network technique for improving the accuracy of scatterometer winds in rainy conditions," *IEEE Trans. Geosci. Remote Sens.*, vol. 48, no. 8, pp. 3114–3122, Aug. 2010.
[18] Y. Troitskaya, D. Sergeev, A. Kandaurov, G. Baidakov, M. Vdovin, and V. Kazakov, "Laboratory and theoretical modeling of air-sea momentum transfer under severe wind conditions," *J. Geophys. Res., Oceans*, vol. 117, Jun. 2012, Art. no. C00J21, doi: 10.1029/2011JC007778.
[19] Y. Troitskaya *et al.*, "Laboratory study of cross-polarized radar return under gale-force wind conditions," *Int. J. Remote Sens.*, vol. 37, no. 9, pp. 1981–1989, Feb. 2016, doi: 10.1080/01431161.2016.1160301.
[20] Y. Troitskaya *et al.*, "Cross-polarization GMF for high wind speed and surface stress retrieval," *J. Geophys. Res., Oceans*, vol. 123, no. 8, pp. 5842–5855, Aug. 2018, doi: 10.1029/2018JC014090.
[21] P. W. Vachon and J. Wolfe, "C-band cross-polarization wind speed retrieval," *IEEE Geosci. Remote Sens. Lett.*, vol. 8, no. 3, pp. 456–459, May 2011.
[22] B. A. Williams and D. G. Long, "Estimation of hurricane winds from seawinds at ultrahigh resolution," *IEEE Trans. Geosci. Remote Sens.*, vol. 46, no. 10, pp. 2924–2935, Oct. 2008.
[23] G. O. Young, "Synthetic structure of industrial plastics," in *Plastics*, J. Peters, Ed., vol. 3, 2nd ed., New York, NY, USA: McGraw-Hill, 1964, pp. 15–64.
[24] S. Yueh, B. W. Stiles, and W. T. Liu, "QuikSCAT wind retrievals for tropical cyclones," *IEEE Trans. Geosci. Remote Sens.*, vol. 41, no. 11, pp. 2616–2628, Nov. 2003.
[25] G.-J. van Zadelhoff, A. Stoffelen, P. W. Vachon, J. Wolfe, J. Horstmann, and M. B. Rivas, "Scatterometer hurricane wind speed retrievals using cross polarization," *Atmos. Meas. Tech. Discuss.*, vol. 7, no. 2, pp. 7945–7984, Aug. 2013, doi: 10.5194/amtd-6-7945-2013.
[26] A. Zavadsky and L. Shemer, "Characterization of turbulent air flow over evolving water-waves in a wind-wave tank," *J. Geophys. Res., Oceans*, vol. 117, Jun. 2012, Art. no. C00J19, doi: 10.1029/2011JC007790.
[27] B. Zhang and W. Perrie, "Cross-polarized synthetic aperture radar: A new potential measurement technique for hurricanes," *Bull. Amer. Meteorol. Soc.*, vol. 93, no. 4, pp. 531–541, Apr. 2012, doi: 10.1175/BAMS-D-11-00001.1.

Olga Stanislavovna Ermakova was born in Nizhny Novgorod, Russia, in 1983. She received the B.S. and M.S. degrees in radiophysics from Nizhny Novgorod State University, Nizhny Novgorod, Russia, in 2005 and 2007, respectively, and the Ph.D. degree in atmospheric and oceanic physics from the Institute of Applied Physics of the Russian Academy of Sciences (RAS), Nizhny Novgorod, Russia, in 2010.

From 2004 to 2007, she was a Research Assistant, from 2007 to 2010, a Junior Researcher, and since 2010, a Researcher with the Institute of Applied Physics RAS. She is the author of more than 20 articles. Her research interests include the investigation of the atmosphere and ocean boundary layers interaction at hurricane wind conditions and the development of wind speed retrieval methods due to the ocean surface remote sensing.

Daniil Alexandrovich Sergeev was born in Nizhny Novgorod, Russia, in 1980. He received the B.S. and M.S. degrees in physics from Nizhny Novgorod State University, Nizhny Novgorod, Russia, in 2001 and 2003, respectively, and the Ph.D. degree in atmospheric and oceanic physics from the Institute of Applied Physics of the Russian Academy of Sciences (RAS), Nizhny Novgorod, Russia, in 2006.

From 2000 to 2007, he was a Junior Researcher, from 2007 to 2008, a Researcher, and in 2008, he became a Senior Researcher with the Institute of Applied Physics RAS. He is the author of five inventions and more than 70 articles. His research interests include the experimental modeling of geophysical currents and investigation of microwave scattering from the wavy ocean surface.

Nikita Sergeevich Rusakov was born in Dzerzhinsk, Russia, in 1995. He received the B.S. and M.S. degrees in radiophysics from Nizhny Novgorod State University, Nizhny Novgorod, Russia, in 2017 and 2019, respectively.

Since 2017, he has been a Research Assistant with the Institute of Applied Physics of the Russian Academy of Sciences (RAS), Nizhny Novgorod, Russia. He is the author of more than ten articles. His research interests include the investigation of radar scattering mechanisms from the wavy water surface and signal processing.

Evgeny Ivanovich Poplavsky was born in Dzerzhinsk, Russia, in 1995. He received the B.S. and M.S. degrees in radiophysics from Nizhny Novgorod State University, Nizhny Novgorod, Russia, in 2017 and 2019, respectively.

Since 2017, he has been a Research Assistant with the Institute of Applied Physics of the Russian Academy of Sciences (RAS), Nizhny Novgorod, Russia. He is the author of more than ten articles. His research interests include the development of algorithms for retrieval of atmospheric geophysical parameters from satellite data and field measurements at high winds.

Galina Nikolaevna Balandina was born in Nizhny Novgorod, Russia, in 1954. She received M.S. degree in radio engineering from Nizhny Novgorod Technical University, Nizhny Novgorod, Russia, in 1976.

From 1976 to 1982, she was an Engineer with the Research Institute for Physics and Technology, Dolgoprudny, Russia. Since 1982, she has been a Leading Programmer with the Institute of Applied Physics of the Russian Academy of Sciences (RAS), Nizhny Novgorod, Russia. She is the author of more than 50 articles. Her research interests include the development of computer software for satellite image processing and program packages for the processing of geophysical currents optical images.

Yuliya Igorevna Troitskaya was born in Nizhny Novgorod, Russia, in 1961. She received the M.S. degree in radiophysics from the Nizhny Novgorod State University, Nizhny Novgorod, Russia, in 1983, and the Ph.D. degree in atmospheric and oceanic physics and the D.Sc. degree from the Institute of Applied Physics of the Russian Academy of Sciences (RAS), Nizhny Novgorod, Russia, in 1987 and 1998, respectively.

From 1987 to 2003, she was a Researcher, Senior Researcher, and Leading Researcher, and in 2003, she became the Head of the Nonlinear Geophysical Processes Department, Institute of Applied Physics RAS. Since 1998, she has been a Professor with the Nizhny Novgorod State University. She is the author of more than 140 articles. Her research interests include the investigation of waves, currents, and turbulence dynamics in the atmosphere and hydrosphere and the development of remote sensing methods for ocean surface investigation.